UDC 621.391.812.62.029.55
Indexing Terms: Radio transmission, propagation effects, ionosphere

Oblique h.f. radiowave propagation in the main trough region of the ionosphere

M. LOCKWOOD, B.Sc., Ph.D.*
and
V. B. MITCHELL, B.Sc., Ph.D.†

SUMMARY
The propagation of 7·335 MHz, c.w. signals over a 5212 km sub-auroral, west-east path is studied. Measurements and semi-empirical predictions are made of the amplitude distributions and Doppler shifts of the received signals. The observed amplitude distribution is fitted with one produced by a numerical fading model, yielding the power losses suffered by the signals during propagation via the predominating modes. The signals are found to suffer exceptionally low losses at certain local times under geomagnetically quiet conditions. The mid-latitude trough in the F2 peak ionization density is predicted by a statistical model to be at the latitudes of this path at these times and at low K_p values. A sharp cut-off in low-power losses at a mean K_p of 2·75 strongly implicates the trough in the propagation of these signals. The Doppler shifts observed at these times cannot be explained by a simple ray-tracing model. It is shown however, that a simple extension of this model to allow for the trough can reproduce the form of the observed diurnal variation.

* *Formerly at the University of Exeter; now with the Appleton Laboratory, Ditton Park, Slough, Berkshire SL3 9JX*

† *Department of Physics, University of Exeter, Stocker Road, Exeter, Devon EX4 4QL.*

1 Introduction

The 'mid-latitude' or 'main' trough in nocturnal F-layer ionization densities was first observed in topside sounder data from the *Alouette 1* sounder[1]. The trough has since been found to be a regular feature of the topside ionospheres of both hemispheres (unlike the shorter-lived polar troughs which are also observed), having a 95% occurrence frequency at local midnight.[2] The trough is seen as a sharp decrease in the ionization density which is of the order of 10 degrees of latitude wide, and which lies along a geomagnetic latitude which varies approximately linearly with the K_p index value[3]. The F-layer peak is typically reduced by a factor of about four at the trough centre.[4] The trough moves equatorward and becomes much narrower at higher K_p values, giving it much steeper walls. The morphology of the trough under quiet conditions has been reviewed by Mendillo and Chacko.[5]

The trough is also observed in total electron content measurements[6] hence it is a depletion, and not a redistribution, of plasma. Very few direct observations of the trough below the F2 peak have been possible. The trough cannot be seen by ground-based ionosondes, due to the effects of off-vertical reflections, except at times of very low geomagnetic activity when the trough is at its widest.[7] The bottomside trough has been observed by various other direct methods including: ion trap experiments;[8] incoherent scatter radar[9] and an ionosonde with direction-finding capabilities.[10] Its presence, and in particular that of its steep poleward wall, have been inferred from various 'oblique echoes' on vertical ionograms by Stanley.[11] Some of the relatively scarce observations of the trough by ground-based and airborne h.f. experiments have been reviewed by Hartmann.[12]

The signals studied in the work described here are propagated along a path that lies approximately geomagnetically west to east at the latitudes at which the trough is observed under quiet magnetic conditions.

2 Amplitude Distributions of the Received Signals

2.1 Observed Distributions

The c.w. signals are transmitted from CHU, Ottawa (geographic co-ordinates: 45°18′N, 75°45′W) at a frequency of 7·335 MHz, with a power of 10 kW and by a vertical monopole antenna. They were received on a Beverage antenna at the Norman Lockyer Observatory, Sidmouth (geographic co-ordinates: 50°41′N, 3°13′W), a great circle distance of 5212 km from the transmitter. A receiver bandwidth of 1 kHz was used and the measured input signal amplitude calibrated frequently against known signal levels to allow for the receiver a.g.c. The amplitude was digitized and then recorded by a mini-computer data-logger. The receiver, data-logger and calibration signal synthesizer were all housed in separate buildings, about 100 m apart to prevent any mutual

0033-7722/80/110559+08 $1.50/0

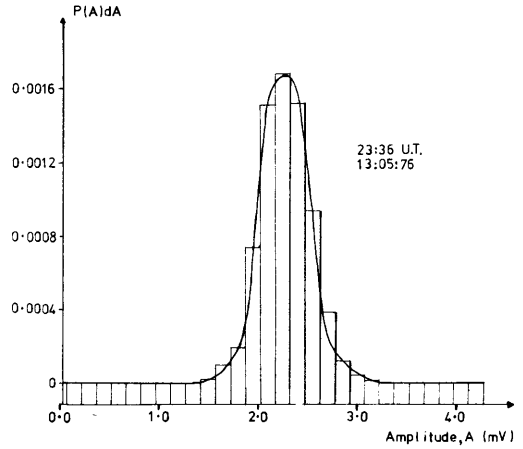

Fig. 1. Histogram of observed probability, $P(A)\mathrm{d}A$ (averaged over 0·15 mV ranges for a $\mathrm{d}A$ of 0·001 mV) as a function of amplitude A. The continuous curve is the model distribution for a single coherent signal of amplitude 2·2 mV (equivalent to a total loss of 113 dB) and random phase scattered signals.

interference problems. The amplitude was sampled at regular intervals from a clock based on the 60kHz transmission from Rugby. The recordings consisted of 512 samples taken first at 500 samples per second and then a further 512 samples taken at a sampling rate of 4 per second. The recordings thus lasted just over 2 minutes and were made at 36 minutes past each hour. The numbers of the 'slow' (4 per second) samples falling in certain amplitude intervals during a recording were counted (after a correction to allow for the time-constants of the receiver a.g.c.) and gave amplitude distributions of which examples are shown in the histograms of Figs. 1 and 2.

From the continuous recordings which were made in a three-month period (April, May and June 1976), 79% had to be discarded as the signals were below the noise level. This was usually due to large non-deviative absorption when all or part of the path was under daytime conditions. A further 12% of the recordings could not be analysed as they yielded amplitude distributions which were broad and complex. This was caused by severe multi-path conditions at the time of the recording, or by large variations in the received power spectrum during the recording. Therefore only 9% of all the recordings could be analysed, a total of 77.

2.2 Model Distributions

The amplitude and phase of the resultant of two interfering signals of different amplitudes and Doppler shifts are given by equations derived by Toman.[13] To this resultant a third signal can be added at that time, t, using the same equations. In this way n specular, coherent signals and a Rayleigh-distributed vector (the scattered signal component) can be added together at the time t. (The resultant of n Rayleigh-distributed vectors is itself a Rayleigh-distributed vector.[14]) This is repeated at different values of t until the resultant phase and amplitude variation in a whole number of beat periods is obtained. The amplitude distribution in a whole number of beat periods can thus be modelled. Adding various r.m.s. scattered components to a single coherent signal yields the well-known Rice–Nakagami distribution,[15, 16] although fluctuations of the coherent component amplitude cause deviations from this.[17] The distribution for the interference of two coherent signals (of amplitudes W_1 and W_2) with various r.m.s. scattered components (W_s) are shown in Fig. 3. It can be seen that here the presence of a second coherent signal gives a second peak in the distribution which can be resolved only if the secondary signal is larger than about three times the r.m.s. scattered signal. Distributions produced by this numerical fading model were fitted to the observed distributions using a chi-squared fit.

Examples of best-fit distributions are shown by the continuous curves in Figs. 1 and 2.

3 Power Losses

The maximum power losses of the resolvable signals, L_{TO}, were evaluated from the signal amplitudes used in the production of the best-fit distribution by using the minima of the measured feeder losses. Figure 4 shows n, the number of observations of L_{TO} in 1dB ranges. It can be seen that in 33 of the usable 77 recordings in this period L_{TO} was less than L_{min}, the minimum loss for a hypothetical link using the same apparatus but over a free-space, straight-line path of length equal to that of the Ottawa–Sidmouth great circle arc. Figure 5 shows an identical histogram for measurements taken with the same apparatus during this period when monitoring signals received from Tirane, Albania.

For this second path, which lies nearly north-south, the L_{TO} value was less than L'_{min} in only four out of a total of 71 usable recordings. Thus the anomalously low losses observed on the Ottawa–Sidmouth path cannot be due to measurement or calibration errors at the receiver as these would also cause anomalously low losses to be observed on the Tirane–Sidmouth path.

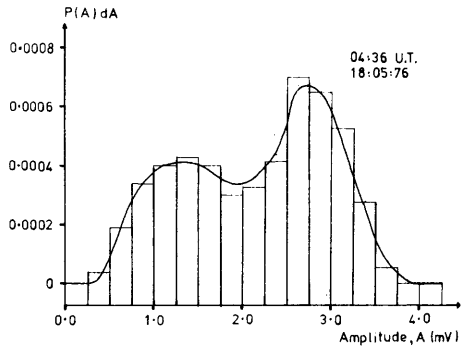

Fig. 2. Histogram of observed probability, $P(A)\mathrm{d}A$ (averaged over 0·25 mV ranges for a $\mathrm{d}A$ of 0·001 mV) as a function of amplitude A. The continuous curve is the model prediction for two coherent signals of amplitudes 2·0 and 1·1 mV (equivalent to total path losses of 114 dB and 123 dB respectively).

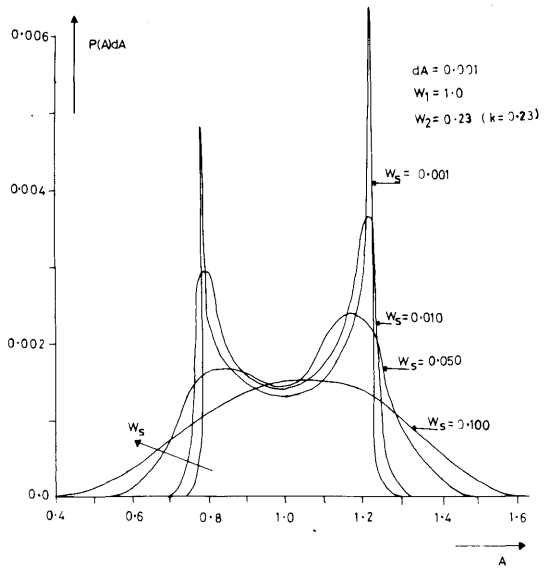

Fig. 3. Probability, $P(A)\mathrm{d}A$ (for a $\mathrm{d}A$ of 0.001 mV), as a function of amplitude A, for two coherent signals of amplitude 1·0 mV and 0·23 mV and various r.m.s. scattered components, W_s.

L_{min} is a minimum possible loss for the path as it is the sum of the minimum of the spatial attenuation, the minimum of the feeder losses and the maxima of the two antenna gains. Hence there are a large number of other factors not included in L_{min} which cause the loss for any one mode of propagation to be considerably greater than L_{min}, for example: absorption losses; polarization losses; reflection losses; additional spatial attenuation (as the ray path length of any ionospheric mode must be greater than the great circle arc length). Semi-empirical predictions of the power loss for the possible modes of propagation were made using a method based on that of Barghausen *et al.*[18] Such predictions are based on monthly means of ionospheric parameters and it is well known that they can differ greatly from the actual losses at any one time. This is due to: approximations used in making the prediction; the large spreads in the values of the parameters used (due to the variability of F-layer propagation), and factors which are not allowed for in the prediction at all. The first two of these possibilities were eliminated from the analysis by evaluating a minimum loss for each propagation mode, L_M. This was done by using a minimum of each loss term in the expression for the total loss (evaluated by using the relevant decile values), and by omitting some other loss terms completely (e.g. deviative absorption and polarization losses). The only gain factors included were focusing due to a spherical ionosphere and maxima of the antenna gains. It was thus possible to get estimates of the 'additional' gain of the observed signals over the minimum predicted loss.

As the predicted loss was minimised this gives a minimum of the additional gain, G_{min}, given by

$$G_{min} = L_M - L_{TO}. \quad (1)$$

Figures 6 and 7 show the predicted field strengths (for isotropic antennae) and elevation angles at the receiver for the modes predicted to be present for median, upper and lower decile nocturnal ionospheres for May 1976. The sum of the transmitter and receiver antenna gains, $(G_T + G_R)$, is shown in Fig. 8 as a function of elevation angles (at both antennae), ϕ, for propagation in the great circle plane. (These curves only strictly apply to propagation via a spherically stratified ionosphere.) These antenna gains were modelled theoretically using a range of ground conditions applicable to the sites in question[19] and then checked by direct calibration over the low elevation angle range used in this experiment.

Figures 6, 7 and 8 show that the predicted dominant propagation mode is the 2F2 mode during these nights, as it always suffers the lowest transmission loss and has the highest total antenna gain. High and low angle

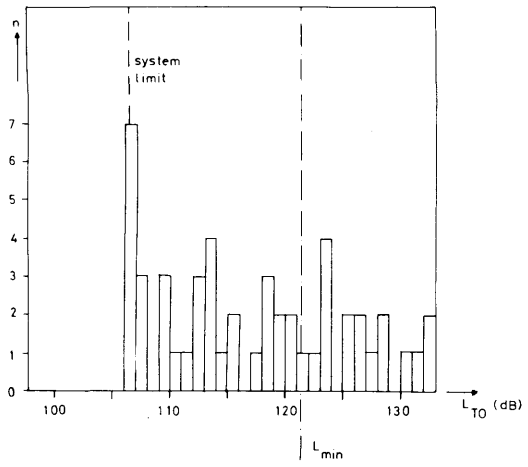

Fig. 4. Histogram of n, the number of observations for which the observed loss on the Ottawa–Sidmouth path is between L ($L_{TO}+1$) dB in April, May and June 1976. L_{min} is the minimum loss of hypothetical link using the same apparatus over a straight-line path of length 5212 km.

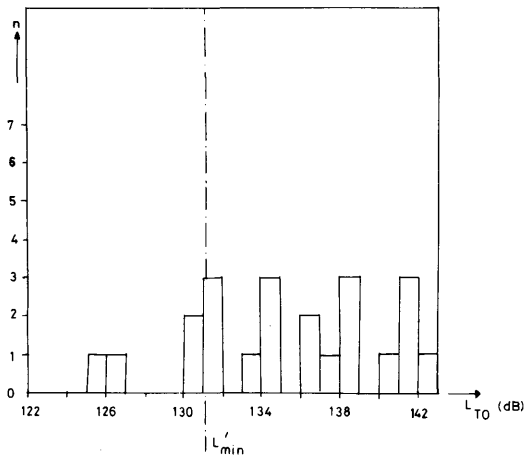

Fig. 5. Histogram of n, the number of observations for which the observed loss on the Tirane–Sidmouth path is between L_{TO} and ($L_{TO}+1$) dB in April, May and June 1976. L'_{min} is the minimum loss of a hypothetical link using the same apparatus over a straight-line path of length 2048 km (the Tirane–Sidmouth great circle distance).

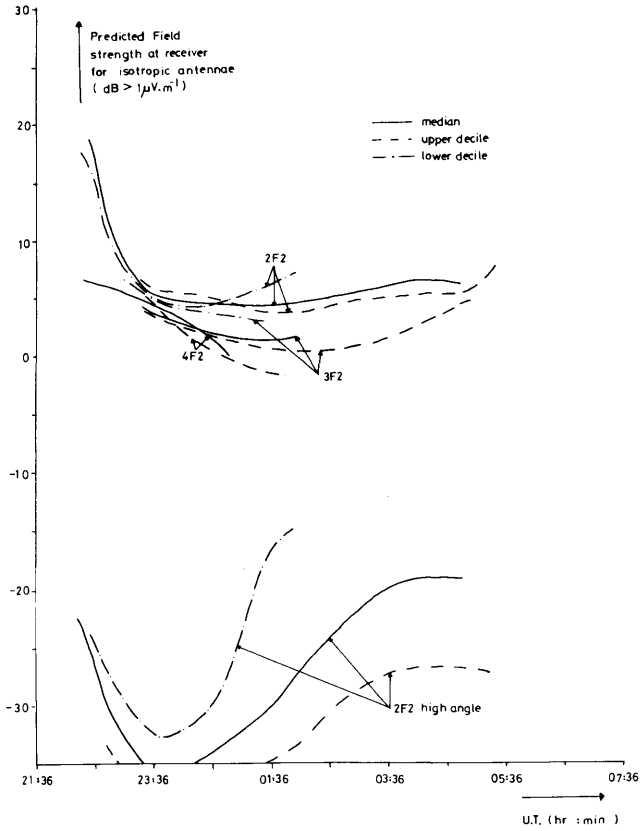

Fig. 6. Field strength at the receiver (for isotropic antennae) for the propagation modes predicted for median, upper and lower decile nocturnal ionospheres in May, 1976.

modes were predicted but only the simplest of mixed modes (1F, 1E and 1E, 1F).

The variations in the calculated values of G_{min} are shown in Fig. 9 for five consecutive days. It can be seen that in this time positive values of G_{min} were often observed during the night. Large positive values were very rarely observed in isolation, rather they were usually part of a regular variation of the type shown by days 1, 2 and 5 of Fig. 9. On days 3 and 4 no G_{min} values in excess of -40 dB were found. In April, May and June 1976 (the period used to compile Fig. 4) values of G_{min} up to $+35$ dB were observed. In 27 of the usable 77 recordings in this period G_{min} was greater than $+10$ dB and in 43 it was positive.

4 Discussion of the Amplitude Results

In a few recordings in the 3-month period the amplitude distribution of the signal received over the west-east path was of a form that could be fitted with a model prediction and that yielded a positive value of G_{min}. Such examples account for only 5% of the total number of recordings made during this period, but this is over half of the 9% of usable recordings. 40% of the recordings taken when the path was totally in darkness were found to be usable. For the north-south path, by way of comparison, only 3% of the usable recordings gave positive G_{min} values and none gave it to be larger than

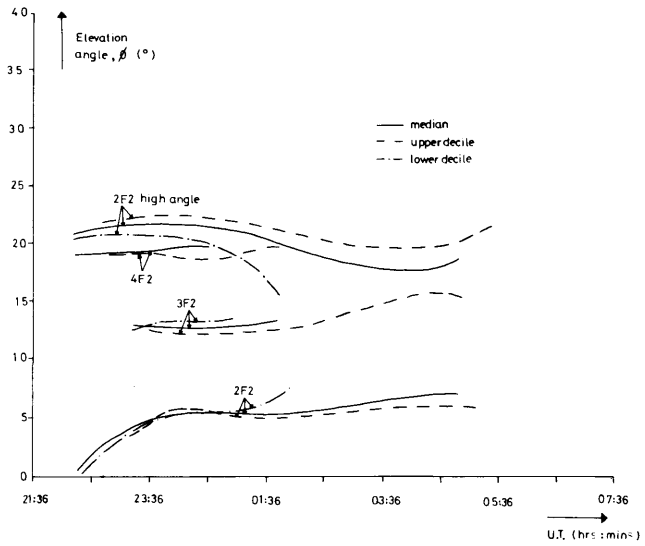

Fig. 7. Elevation angles at the receiver for modes shown in Fig. 6.

$+7$ dB (compared with 43% of usable recordings on the west-east path for which G_{min} exceeds this value).

By using the definition of G_{min} given in equation (1) there are only a few possible causes of any positive G_{min} values. Firstly, the propagation may be due to a mode deemed impossible by the prediction scheme. The most important candidate for this is the high angle 1F2 mode, which the prediction scheme does not consider over such long paths, but which has been observed to propagate over a similar path by Warren and Hagg and by Kift.[20] Muldrew and Maliphant[21] showed by ray tracing that such propagation was possible and observed one-hop

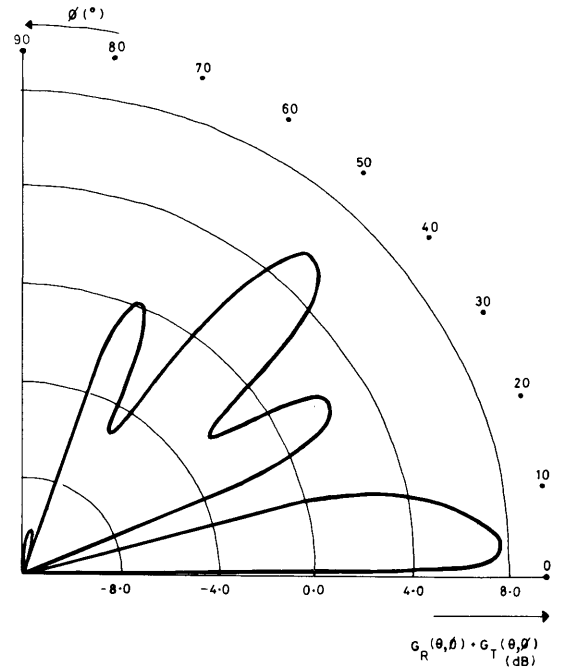

Fig. 8. Sum of receiver and transmitter antenna gains as a function of elevation angle, ϕ, modelled for great circle propagation and equal elevation angles at receiver and transmitter.

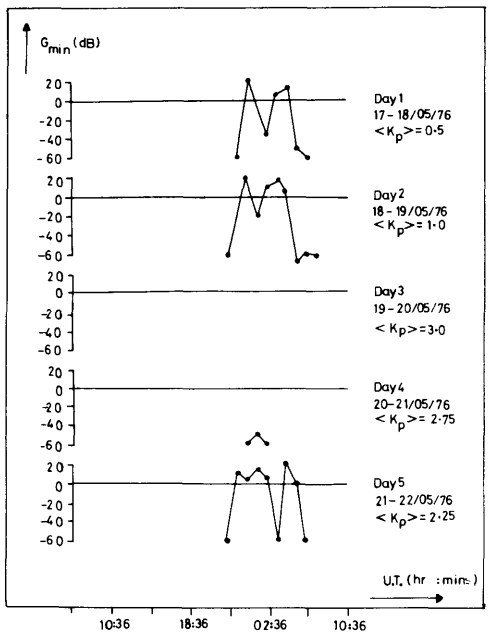

Fig. 9. The variation of the additional ionospheric gain of the predominating mode, G_{min}, during five consecutive days.

propagation to be present on average 35% of the time two-hop propagation was present on an Ottawa–Hague path. In the summer this ratio rose to 80–90%. However they only observed the one-hop mode at frequencies above 4 or 5 MHz below the m.u.f.; (Warren and Hagg's measurement was also at 27–33 MHz). The absolute lower frequency limit of the high angle one-hop mode was shown to be the layer critical frequency for certain simple models. Thus the frequency of these signals is lower than those for which Pedersen one-hop has been observed. Such a mode would also have a lower antenna gain than the 2F2 mode (Fig. 8) and suffer larger deviative absorption and divergence losses (although the latter can be reduced by an increase in the layer thickness[22]).

Another possibility arises from the 'maximum range' focusing effect on long hops caused by a continuous increase in the ionization between the E and F-layers. This effect is usually not present at night due to the deeper valley between the layers.[23] Positive G_{min} values may also be due to modes which have not been resolved by the amplitude distribution. This would be the case for signals which had Doppler shifts differing by less than the inverse of the recordings duration (i.e. less than about 0·01 Hz). However large numbers of such signals, all in phase at the time of recordings, are needed to explain the magnitude of the G_{min} values, a situation which is statistically improbable.

Other factors which could contribute to positive G_{min} values are focusing due to tilts of the iso-ionic contours of the ionosphere, and tilt-supported 'chordal' ('supertrapezoidal') propagation modes as are observed in trans-equatorial propagation.[24] Such modes involve two reflections from an ionospheric layer without an intermediate reflection by the ground or by the topside of a lower layer.

Hence it appears possible that tilts may play a large role in the propagation of these signals. Large tilts of the F-layer are expected near the latitudes of this path at the walls of the mid-latitude trough. In order to evaluate their possible role in the propagation of these signals results were used concerning the mean morphology of the trough. Various such statistical models of the trough (as a function of local time, season, K_p index and sunspot number) have been compiled from the existing data.[25-27] It must be remembered that there are several pitfalls in the use of such statistical morphological results[4] and the regression equations cannot be used to predict the actual boundary locations of the trough at any one instant.[28] Hence their use here can only indicate that any one hypothesis is consistent with the mean statistical position of the trough.

Consider two points, A and B, situated at an altitude of 200 km, one-quarter and three-quarters of the way along the Ottawa–Sidmouth arc. The reflection points of the 2F2 mode will in general be removed from A and B, but they can be regarded as sufficiently accurate indicators considering the uncertainties in the predicted trough wall positions. The trough depletion is not very large during the day as then photoionization dominates over the loss mechanisms which are responsible for the trough's formation. Hence at dusk the trough 'opens' with increasing local time and it 'closes' at dawn giving sunset and sunrise 'end walls' to the trough as viewed in a LT—invariant latitude plot. The mean times that the trough begins and ceases opening and closing at the points A and B can be calculated for any one night from the solar zenith angles and the K_p index value using the regression equations given by Feinblum.[26] 80% of the observed positive values of G_{min} were at times when the trough was fully open at both A and B, 89% were at times when the trough was at least partially opened at both A and B and all were within an hour of these times. The times between which the trough opened at A and closed at B varied with the K_p index in exactly the same way as the times that positive G_{min} values began and ceased respectively. The two maxima in G_{min} were also at times when A and B were nearest to the end walls. This is qualitatively consistent with the idea of a 2F2 mode focused by the trough because at these times focusing would occur in the elevational plane as well as the azimuthal plane.[7] To test if this hypothesis can explain the magnitudes of the G_{min} values quantitatively requires a three-dimensional ray tracing study of propagation along the length of the trough.

Figure 10 shows the invariant latitudes of the equatorward and poleward edges of the trough walls as a function of local time for thee K_p values. These are given by the regression equation given by Halcrow and

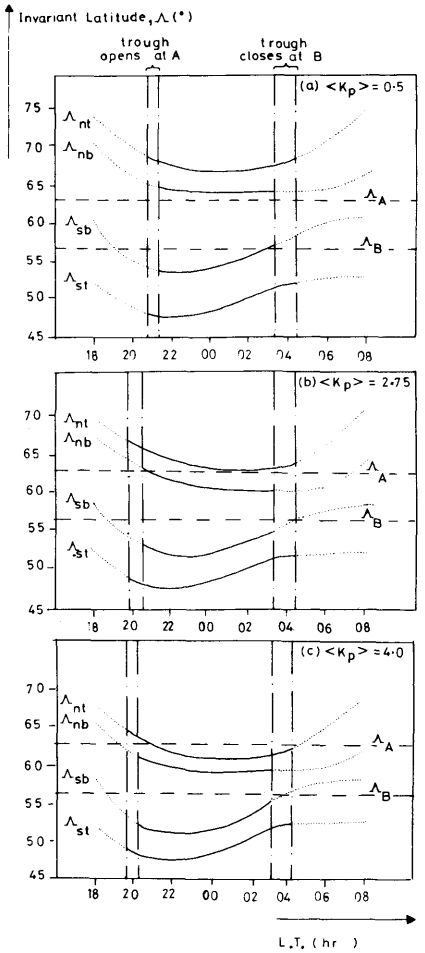

Fig. 10. The invariant latitudes of the tops and bases of the north and south troughwalls (Λ_{nt}, Λ_{nb}, Λ_{st} and Λ_{sb} respectively) of the northern hemisphere trough for 17–18/05/76 and for mean K_p values of (a) 0·5, (b) 2·75 and (c) 4·0.

Nisbet[4] from 8 years' *Alouette I* and *II* data. Also shown are the invariant latitudes of the points A and B, Λ_A and Λ_B. It can be seen that under quiet magnetic conditions both points are within the trough walls at the times at which the trough would be open at them. As K_p increases the trough moves equatorward, especially its poleward wall, making it narrower and equatorward of the point A, B remains within the trough wall at all K_p at these times. Hence at low K_p all the path is at the latitudes of the trough. In days 3 and 4 of Fig. 9 no large values of G_{min} were observed. On these two days the mean K_p is significantly higher. Figure 11 shows the observed values of G_{min} in April, May and June 1976 as a function of the mean K_p on the day of recording. The daily mean of the K_p value (from 12 UT to 12 UT) was used because the plasmapause, and hence the trough, positions are determined by the K_p history as well as its current value.[28] It can be seen that G_{min} is more consistently higher at the lowest K_p values, 80% at mean K_p less than 1·0 giving positive G_{min} values; this falls to 60% for mean K_p in the range 1·0 to 3·0 and for K_p greater than 3·0 it is zero. No positive G_{min} values are observed at all when the mean K_p exceeds 2·75, there being a sharp cut-off in large G_{min} about this value. In Fig. 10(b) it can be seen that at this K_p the point A lies within the poleward trough wall for most of the night. At lower K_p, A is inside the trough and at higher K_p it is outside it. This, again, qualitatively suggests the trough is focusing a mode. For example in a two-hop mode the first hop would be focused at low K_p but defocused at higher values, giving a cut-off in G_{min} at 2·75 as observed. It is unlikely that the 42% of recordings at mean K_p below 2·75 which yield negative G_{min} are due to the absence of a bottomside trough as the topside trough is present on roughly 95% of all nights.[2] These values are more likely to be due to the losses minimized in calculating G_{min} (e.g. non-zero polarization losses, auroral absorption, etc).

5 Doppler Shifts

The local oscillators used at the receiver and transmitter have a frequency stability in excess of 1 part in 10^9. This is the principal limitation on the accuracy of the Doppler shift measurement and corresponds to an error of less than $\pm 0{\cdot}01$ Hz on these signals.

The measurement of the Doppler shift of oblique h.f., c.w. waves was first done by Essen in 1935.[29] He viewed the ionospheric shift as an error in standard frequency transmissions, rather than as a source of information on the ionosphere. The technique developed into the latter as the accuracy of local oscillators increased and data storage techniques improved (e.g. Watts and Davies[30]). Full analysis of Doppler shifts is complicated by various effects, even at vertical incidence.[31] The simplest model

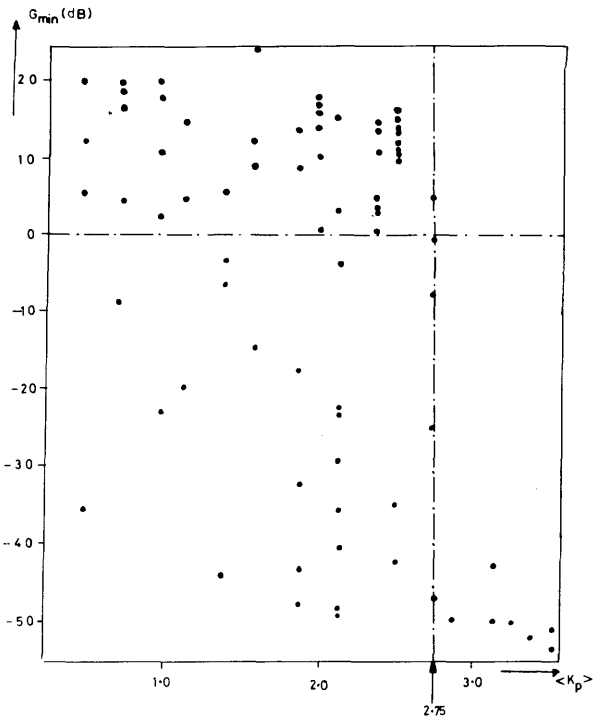

Fig. 11. Observed values of G_{min} in April, May and June, 1976, as a function of the mean K_p value.

for very oblique signals is a mirror-like reflecting ionosphere moving vertically. This model gives a shift which is proportional to the signal frequency, the layer velocity and the cosine of the angle of incidence of the rays onto this mirror-like layer. Hence shifts are smaller for longer paths.

The received signals were mixed down with signals derived from the local oscillator and their phase compared with that of another signal derived from the local oscillator. This phase comparison was done digitally by timing the delay between the zero crossovers of the two signals. The rate of change of this phase difference yields the Doppler shift of the composite sky wave. This equals the Doppler shift of the dominant mode, Δf, when averaged over a whole number of beat periods.[13] The mean shift in a 2-minute period was recorded hourly in the same way as was the amplitude, immediately prior to the amplitude recording.

An example of the observed Doppler shift variation is shown by the points in Fig. 12. Shifts could only be observed when G_{min} was large (approximately greater than -10 dB for midnight at the receiver) as the Doppler measuring system was designed to be triggered only by signals above a certain level. The Doppler variations always showed a regular diurnal variation of the kind seen in Fig. 12. This has features similar to the observed G_{min} variations in that it showed two maxima during a night with an intermediate minimum. The second peak is surprisingly large, being of amplitude between 0·2 and 0·5 Hz and occurring between 04 and 06 UT.

These Doppler shift results cannot be explained easily without involving the mid-latitude trough. The curves in Fig. 12 are produced by two-dimensional ray tracing through a parabolic F-layer of constant semi-thickness. The layer peak density and height was taken as a function of local time, for the date of the shown recordings, from the world maps used in the propagation loss prediction. This crude model does not explain either the form or the magnitudes of the observed Doppler shift variations (the continuous curve). If however, a trough in the peak density and height are introduced (of the model form used by Halcrow and Nisbet[4]) a variation like the one shown by the dashed curve is produced. In this example the peak density is reduced by a factor of four inside the trough relative to its value outside (after Halcrow and Nisbet[4]), the peak height is increased by 40 km and the semi-thickness is kept constant. It can be seen that this curve is considerably closer to the observed values. It is interesting to note that in the ray-tracing prediction the predominating mode was initially a two-hop mode, the angle of incidence at the ground reflection then became larger until that reflection did not occur at all. After this the mode was thus a 'chordal' type mode. The amount by which the ray 'missed' the Earth's surface between the two-layer

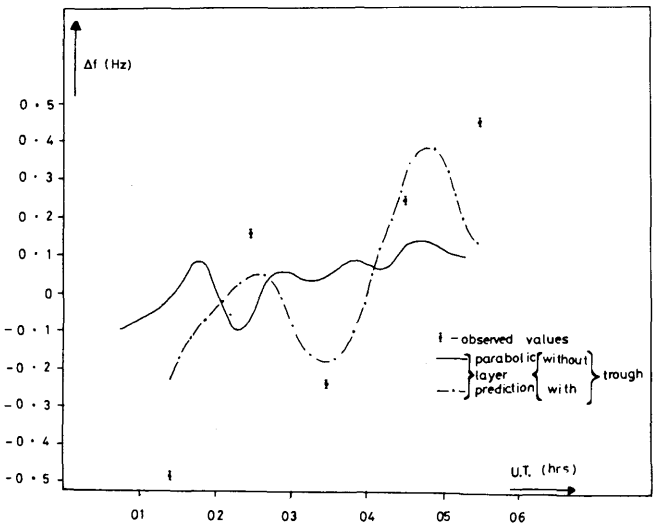

Fig. 12. Observed Doppler shift variation or 05–06/06/77 (mean $K_p = 1{\cdot}6$). The continuous line is a ray tracing model prediction with no allowance for the mid-latitude trough. In the dashed curve a trough model has been included in the prediction.

reflections firstly increased but then began to decrease until the conventional two-hop mode, with a ground reflection, was restored.

6 Conclusions

The presence of anomalously low power losses on a path which lies along the length of the mid-latitude trough and their absence from a path which lies nearly perpendicular to it, suggests it may be affecting the propagation of radio waves over the former path. The trough is strongly implicated by the cut-off in low power losses at the mean K_p when the path would, on average, no longer be entirely within the trough. The times of observations of low losses vary with K_p in agreement with the times that the trough opens and closes in the regions of ionospheric reflection of a 2F mode. Further evidence comes from the Doppler shift measurements which reveal exceptionally large, regular shifts at these times. The shifts can be modelled easily only if a crude model of the trough is introduced. This suggests the trough is supporting a low-loss 2F2 mode or a 'chordal' hop type mode at these times.

7 Acknowledgments

The authors are grateful to the staff of the Radio and Navigation Department, Royal Aircraft Establishment, Farnborough, for their help with the computer predictions. Thanks are also due to the staff of the Radio Research Centre, Auckland University, for their help with the ray-tracing modelling of the Doppler shifts. One of us (M. Lockwood) is indebted to the Science Research Council for a grant under the 'Co-operative Awards in Science and Engineering' scheme.

8 References

1 Muldrew, D. B., 'F region ionisation troughs deduced from Alouette data', *J. Geophys. Res.*, **70**, pp. 2635–50, 1965.
2 Ahmed, M., Sagalyn, R. C., Wildman, P. J. L. and Burke, W. J., 'Topside ionospheric trough morphology: Occurrence frequency and diurnal, seasonal and altitude variations,' *J. Geophys. Res.*, **84**, pp. 489–98, 1979.
3 Köhnlein, W. and Raitt, W. J., 'Position of the mid-latitude trough in the topside ionosphere as deduced from ESRO 4 observations,' *Planet. Space Sci.*, **25**, pp. 600–2, 1977.
4 Halcrow, B. W. and Nisbet, J. S., 'A model of F2 peak electron densities in the main trough region of the ionsphere', *Radio Sci.*, **12**, pp. 815–20, 1977.
5 Mendillo, M. and Chacko, C. C., 'The base level ionospheric trough,' *J. Geophys. Res.*, **82**, pp. 5129–37, 1977.
6 Mendillo, M. and Klobuchar, J. A., 'Investigations of the ionospheric F region using multistation electron content observations,' *J. Geophys. Res.*, **80**, pp. 643–50, 1975.
7 Helms, W. J. and Thompson, A. D., 'Ray tracing simulation of ionisation trough effects upon radio waves,' *Radio Sci.*, **8**, pp. 1125–32, 1973.
8 Sharp, G. W., 'Mid-latitude trough in the night ionosphere,' *J. Geophys. Res.*, **71**, pp. 1345–56, 1966.
9 Taylor, G. N., 'Structure at the poleward edge of the mid-latitude F region trough,' *J. Atmos. Terr. Phys.*, **35**, pp. 647–56, 1972.
10 Bowman, G. C., 'Ionisation troughs below the F2 layer maximum,' *Planet. Space Sci.*, **17**, pp. 777–96, 1969.
11 Stanley, G. M., 'Ground based studies of the F region in the vicinity of the mid-latitude trough,' *J. Geophys. Res.*, **71**, pp. 5067–75, 1966.
12 Hartmann, G. K., 'H.f. and u.h.f. propagation studies of the mid-latitude ionosphere,' *Ann. Geophys.*, **31**, pp. 39–51, 1975.
13 Toman, K., 'Ionospheric phase—and group—path,' *J. Atmos. Terr. Phys.*, **29**, pp. 1019–24, 1967.
14 Norton, K. A., Völger, L. E., Mansfield, W. F., and Short, P. J., 'The probability distribution of the amplitude of a constant vector plus a Rayleigh distributed vector,' *Proc. I.R.E.* **43**, pp. 1354–61, 1955.
15 McNicol, R. W. E., 'The fading of radio waves of medium and high frequencies', *Proc. Instn Elect Engrs*, **96**, pt. 3, pp. 512–24, 1949.
16 Röttger, J., 'Influence of spread F on h.f. radio signals,' AGARD Conference Proceedings No. 173, Paper 26, 1975.
17 Vinogradova, M. B. and Gusev, V. D., 'Amplitude distribution of a scattered field with allowance for the focusing effect of large scale ionospheric inhomogenities,' *Geomag. and Aeron.*, **16**, No. 5, pp. 459–62 1977.
18 Barghausen, A. F., Finney, J. W., Proctor, L. L. and Schultz, L. D., 'Predicting long-term operational parameters of high-frequency sky-wave telecommunication systems,' ESSA Tech. Rept. WRL 1110–ITS 78, USA Govt. Printing Office, Washington, 1969.
19 Travers, D. N., Martin, P. E. and Sherill, W. M., 'Use of Beverage antenna in wide aperture h.f. direction finding,' Rep. Southwest Research Inst., San Antonio, 1964.
20 Kift, F., 'Single hop propagation of radio waves to a distance of 5300 km,' *Nature*, **181**, pp. 1459–60, 24th May 1958.
21 Muldrew, D. B. and Maliphant, R. G., 'Long distance one-hop ionospheric radio wave propagation,' *J. Geophys Res.*, **67**, pp. 1805–15, 1962.
22 Sazhin, V. I. and Tinin, M. V., 'Long distance propagation by means of the Pedersen ray,' *Geomag. and Aeron.*, **15**, pp. 564–5, 1975.
23 Croft, T. A., 'H.F. radio focusing caused by the electron distribution between ionospheric layers,' *J. Geophys. Res.*, **72**, pp. 2343–55, 1967.
24 Yeh, K. C. and Villard, O. G., 'A new type of fading observable on high frequency radio transmissions propagated over paths crossing the magnetic equator,' *Proc. IRE*, **46**, pp. 1968–70, 1958.
25 Halcrow, B. W., 'F2 peak electron densities in the main trough region of the ionosphere,' Tech. Rept. PSU–ILR–IR–55, Ionospheric Research Laboratories, Pennsylvania State University, 1976.
26 Feinblum, D. A., 'Hilion—a model of the high latitude ionospheric F2 layer,' Tech. Rept, US Army Contract No. DAHC–60–71–C–0005, Bell Labs., New Jersey, 1973.
27 Pike, C. P., 'An analytic model of the main F-layer trough,' AFGL–TR–76–0098, Air Force Geophysics Labs., Cambridge, Mass., 1976.
28 Mendillo, M., Chacko, C. C., Lynch, F. and Wildman, P. L. J. 'Attempts to predict trough/plasmapause boundaries in real time,' AFGL–TR–78–0080, p. 105, Air Force Geophysics Labs., Cambridge, Mass., 1978.
29 Essen, L., 'International frequency comparisons by means of standard radio emissions,' *Proc. Roy. Soc.*, **149**, A, pp. 506–10, 1935.
30 Watts, J. and Davies, K., 'Rapid frequency analysis of fading radio signals,' *J. Geophys. Res.*, **65**, pp. 2295–301, 1960.
31 Robinson, L. and Dyson, P. L., 'Effects of ionospheric irregularities on radio waves—I. Phase path changes,' *J. Atmos. Terr. Phys.*, **37**, pp. 1459–67, 1975.

Manuscript first received by the Institution on 23rd March 1978, in revised form on 19th September 1979, and in final form on 15th May 1980. [Paper No. 1960/Comm 258)